

## Energy Dependence of $\Lambda$ and $\bar{\Lambda}$ Production at CERN-SPS Energies

A. Mischke<sup>8</sup> for the NA49 Collaboration

S.V. Afanasiev<sup>9</sup>, T. Anticic<sup>21</sup>, B. Baatar<sup>9</sup>, D. Barna<sup>5</sup>, J. Bartke<sup>7</sup>, R.A. Barton<sup>3</sup>, M. Behler<sup>15</sup>, L. Betev<sup>10</sup>, H. Białkowska<sup>19</sup>, A. Billmeier<sup>10</sup>, C. Blume<sup>8</sup>, C.O. Blyth<sup>3</sup>, B. Boimska<sup>19</sup>, M. Botje<sup>1</sup>, J. Bracinik<sup>4</sup>, R. Bramm<sup>10</sup>, R. Brun<sup>11</sup>, P. Bunčić<sup>10,11</sup>, V. Cerny<sup>4</sup>, O. Chvala<sup>17</sup>, J.G. Cramer<sup>18</sup>, P. Csató<sup>5</sup>, P. Dinkelaker<sup>10</sup>, V. Eckardt<sup>16</sup>, P. Filip<sup>16</sup>, H.G. Fischer<sup>11</sup>, Z. Fodor<sup>5</sup>, P. Foka<sup>8</sup>, P. Freund<sup>16</sup>, V. Friese<sup>8,15</sup>, J. Gál<sup>5</sup>, M. Gaździcki<sup>10</sup>, G. Georgopoulos<sup>2</sup>, E. Gładysz<sup>7</sup>, S. Hegyi<sup>5</sup>, C. Höhne<sup>15</sup>, G. Igo<sup>14</sup>, P.G. Jones<sup>3</sup>, K. Kadija<sup>11,21</sup>, A. Karev<sup>16</sup>, V.I. Kolesnikov<sup>9</sup>, T. Kollegger<sup>10</sup>, M. Kowalski<sup>7</sup>, I. Kraus<sup>8</sup>, M. Kreps<sup>4</sup>, M. van Leeuwen<sup>1</sup>, P. Lévai<sup>5</sup>, A.I. Malakhov<sup>9</sup>, S. Margetis<sup>13</sup>, C. Markert<sup>8</sup>, B.W. Mayes<sup>12</sup>, G.L. Melkumov<sup>9</sup>, C. Meurer<sup>10</sup>, A. Mischke<sup>8</sup>, M. Mitrovski<sup>10</sup>, J. Molnár<sup>5</sup>, J.M. Nelson<sup>3</sup>, G. Pála<sup>5</sup>, A.D. Panagiotou<sup>2</sup>, K. Perl<sup>20</sup>, A. Petridis<sup>2</sup>, M. Pikna<sup>4</sup>, L. Pinsky<sup>12</sup>, F. Pühlhofer<sup>15</sup>, J.G. Reid<sup>18</sup>, R. Renfordt<sup>10</sup>, W. Retyk<sup>20</sup>, C. Roland<sup>6</sup>, G. Roland<sup>6</sup>, A. Rybicki<sup>7</sup>, T. Sammer<sup>16</sup>, A. Sandoval<sup>8</sup>, H. Sann<sup>8</sup>, N. Schmitz<sup>16</sup>, P. Seyboth<sup>16</sup>, F. Siklér<sup>5</sup>, B. Sitar<sup>4</sup>, E. Skrzypczak<sup>20</sup>, G.T.A. Squier<sup>3</sup>, R. Stock<sup>10</sup>, H. Ströbele<sup>10</sup>, T. Susa<sup>21</sup>, I. Szentpétery<sup>5</sup>, J. Sziklai<sup>5</sup>, T.A. Trainor<sup>18</sup>, D. Varga<sup>5</sup>, M. Vassiliou<sup>2</sup>, G.I. Veres<sup>5</sup>, G. Vesztergombi<sup>5</sup>, D. Vranić<sup>8</sup>, S. Wenig<sup>11</sup>, A. Wetzler<sup>10</sup>, C. Whitten<sup>14</sup>, I.K. Yoo<sup>8,15</sup>, J. Zaraneck<sup>10</sup>, J. Zimányi<sup>5</sup>

<sup>1</sup>NIKHEF, Amsterdam, Netherlands.

<sup>2</sup>Department of Physics, University of Athens, Athens, Greece.

<sup>3</sup>Birmingham University, Birmingham, England.

<sup>4</sup>Comenius University, Bratislava, Slovakia.

<sup>5</sup>KFKI Research Institute for Particle and Nuclear Physics, Budapest, Hungary.

<sup>6</sup>MIT, Cambridge, USA.

<sup>7</sup>Institute of Nuclear Physics, Cracow, Poland.

<sup>8</sup>Gesellschaft für Schwerionenforschung (GSI), Darmstadt, Germany.

<sup>9</sup>Joint Institute for Nuclear Research, Dubna, Russia.

<sup>10</sup>Fachbereich Physik der Universität, Frankfurt, Germany.

<sup>11</sup>CERN, Geneva, Switzerland.

<sup>12</sup>University of Houston, Houston, TX, USA.

<sup>13</sup>Kent State University, Kent, OH, USA.

<sup>14</sup>University of California at Los Angeles, Los Angeles, USA.

<sup>15</sup>Fachbereich Physik der Universität, Marburg, Germany.

<sup>16</sup>Max-Planck-Institut für Physik, Munich, Germany.

<sup>17</sup>Institute of Particle and Nuclear Physics, Charles University, Prague, Czech Republic.

<sup>18</sup>Nuclear Physics Laboratory, University of Washington, Seattle, WA, USA.

<sup>19</sup>Institute for Nuclear Studies, Warsaw, Poland.

<sup>20</sup>Institute for Experimental Physics, University of Warsaw, Warsaw, Poland.

<sup>21</sup>Rudjer Boskovic Institute, Zagreb, Croatia.

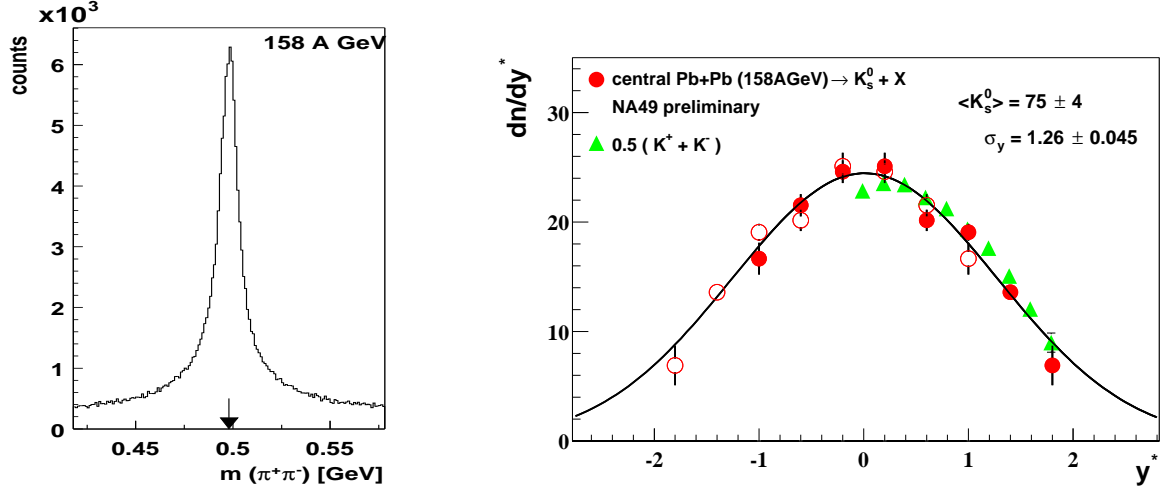


Figure 1. Invariant mass distribution (left) and rapidity distribution (right) of  $K_s^0$  at 158 A·GeV.

Rapidity distributions for  $\Lambda$  and  $\bar{\Lambda}$  hyperons in central Pb-Pb collisions at 40, 80 and 158 A·GeV and for  $K_s^0$  mesons at 158 A·GeV are presented. The lambda multiplicities are studied as a function of collision energy together with AGS and RHIC measurements and compared to model predictions. A different energy dependence of the  $\Lambda/\pi$  and  $\bar{\Lambda}/\pi$  is observed. The  $\bar{\Lambda}/\Lambda$  ratio shows a steep increase with collision energy. Evidence for a  $\bar{\Lambda}/\bar{p}$  ratio greater than 1 is found at 40 A·GeV.

## 1. Introduction

Anomalies in the energy dependence of strangeness production have been predicted as a hint for the onset of deconfinement [1,2]. Since  $\Lambda$  hyperons contain between 30 and 60% of the total strangeness produced in hadronic interactions their measurements allows to study simultaneously strangeness production and the effect of net baryon density.

## 2. Analysis

The data sets used for the present analysis are the 7.2 %, 7.2 % and 10 % most central Pb-Pb events at 40, 80 and 158 A·GeV beam energy, corresponding to 8.73, 12.3 and 17.3 GeV c.m. energy per nucleon nucleon pair. The NA49 experiment [3] identifies neutral strange baryons by reconstructing their characteristic V0 decay topology  $\Lambda \rightarrow p + \pi^-$ ,  $\bar{\Lambda} \rightarrow \bar{p} + \pi^+$  and  $K_s^0 \rightarrow \pi^+ + \pi^-$ . The  $\Lambda$  hyperons contain the short-lived  $\Sigma^0$ , which decay electro-magnetically into  $\Lambda\gamma$ .

The charged decay products are measured with four time projection chambers (TPCs), two of them are located inside two large dipole magnets, the other two downstream of the magnets symmetrically to the beam line [3]. In figure 1, the invariant mass distribution of  $K_s^0$  at 158 A·GeV is shown. An agreement between the peak position and the nominal  $K_s^0$  mass, indicated by the arrow, is observed. The invariant mass distributions of  $\Lambda$  and  $\bar{\Lambda}$  are shown in reference [4]. The mass resolution ( $\sigma_m$ ) is 2 MeV/ $c^2$  for the lambdas and 4 MeV/ $c^2$  for  $K_s^0$ .

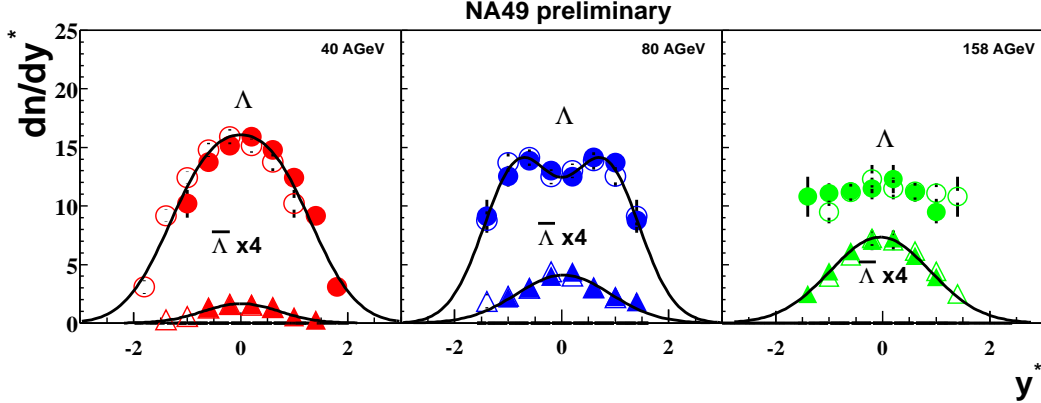


Figure 2. Rapidity distribution of  $\Lambda$  and  $\bar{\Lambda}$  produced in central Pb-Pb collisions at 40 (left), 80 (middle) and 158 A-GeV/u (right). The reflected points (open symbols) are in good agreement with the measured ones (filled symbols).

### 3. Spectra

Corrections, described in detail in reference [4], are applied bin by bin in rapidity and transverse momentum for geometrical acceptance and tracking efficiency. The rapidity distributions are obtained by integrating the measured  $p_T$ -spectra and by extrapolation into unmeasured regions. In figure 2, the rapidity distributions of  $\Lambda$  and  $\bar{\Lambda}$  are summarized for all three energies. It is found that the distribution of the  $\Lambda$  is broader than that of the  $\bar{\Lambda}$ . The  $\Lambda$  rapidity distribution becomes broader with increasing energy. The total lambda baryon multiplicities are obtained by integration of the rapidity spectra with small extrapolations into unmeasured regions using a Gaussian fit for the  $\bar{\Lambda}$  at all three energies and the  $\Lambda$  at 40 A-GeV. A double Gaussian is used for the  $\Lambda$  at 80 A-GeV. For the  $\Lambda$  rapidity distribution at 158 A-GeV an extrapolation is made using realistic estimates of the tails (e.g.  $\Lambda$  from central S+S and net-proton distribution at 158 A-GeV [4]).

The corrections and the analysis procedure were checked by extracting the  $K_s^0$  meson at 158 A-GeV and comparing them to the charged kaons [5]. The charged kaons are identified with a different method (dE/dx). The comparison between the rapidity distribution of  $K_s^0$  and the charged kaons (using isospin symmetry:  $K_s^0 = (K^+ + K^-)/2$ ) is shown in figure 1 (right). Good agreement is observed. The total  $K_s^0$  multiplicity, quantified using a Gaussian fit to extrapolate the unmeasured regions yields  $\langle K_s^0 \rangle = 75 \pm 4$ .

### 4. Energy Dependence

The maximum of the  $\Lambda$  rapidity distribution decreases with increasing collision energy, as shown in figure 2. This effect is even enhanced in the  $\Lambda/\pi$  ratio (see figure 3(a)). The pions are calculated according to  $\pi = 3/2 (\pi^+ + \pi^-)$  [7,5]. The data at AGS energies (triangles) are taken from reference [8–10,12,13]. The  $\Lambda/\pi$  ratio steeply increases at AGS energies, reaches a maximum and drops at SPS energies. In comparison, the  $\bar{\Lambda}/\pi$  ratio shows a monotonic increase up to RHIC energies [11] without significant structure (see figure 3(b)). The same behavior is visible for the total multiplicities  $\langle \Lambda \rangle / \langle \pi \rangle$  and  $\langle \bar{\Lambda} \rangle / \langle \pi \rangle$  as shown in figure 3(c) and (d). These differences can be attributed to different production mechanism for  $\Lambda$  and  $\bar{\Lambda}$  and to the effect of net-baryon density.

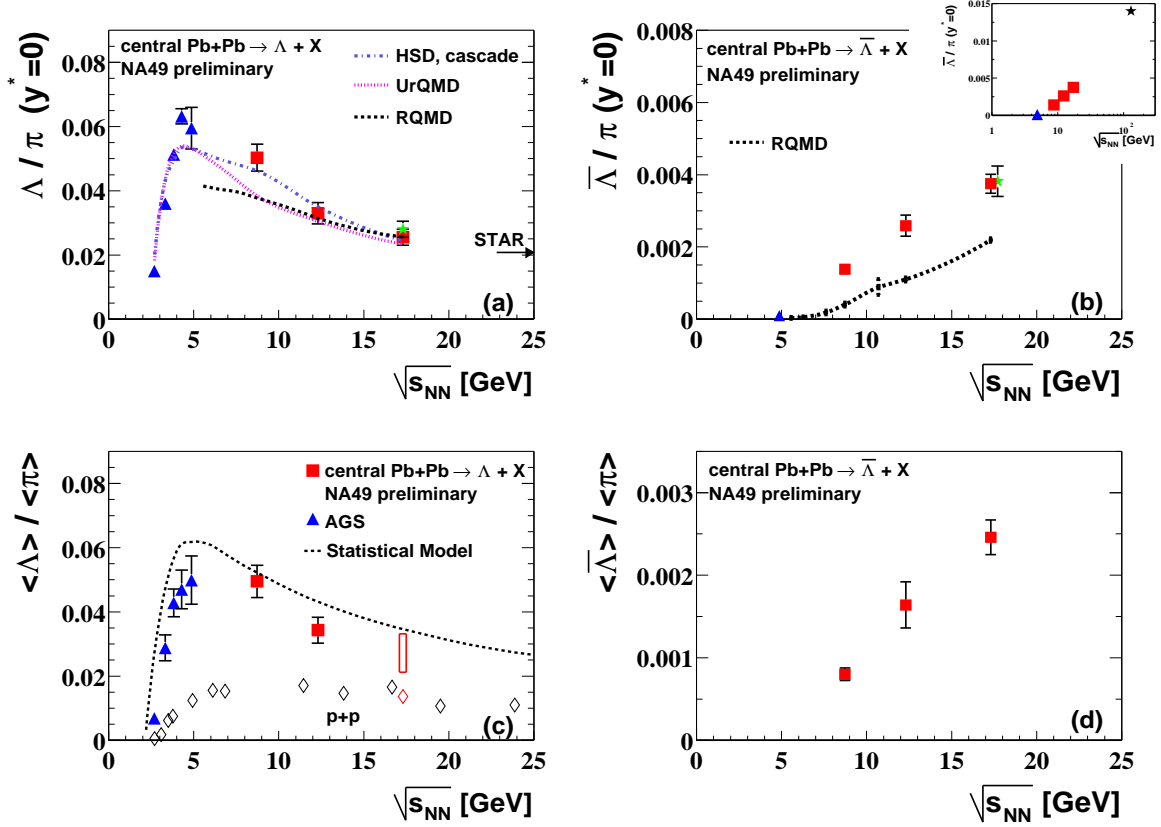


Figure 3. Energy dependence of the  $\Lambda/\pi$  (a) and the  $\bar{\Lambda}/\pi$  (b) at mid-rapidity. In the logarithmic scaled inset of figure (b) the STAR measurement is shown in addition. The same ratios are shown for the  $4\pi$  values (3(c) and (d)). The  $\langle\Lambda\rangle/\langle\pi\rangle$  ratio from p+p collisions at different energies [1,6] is shown as well. The different lines represent different model predictions.

Since the  $K^+$  carry about 80% of the produced  $\bar{s}$  quarks we expect the  $K^+/\pi^+$  ratio to show a similar behavior as the  $\Lambda/\pi$  ratio (using strangeness conservation) which is indeed the case [5].

In figure 3, the measurements are compared to model predictions from UrQMD [14], HSD [15], RQMD [16] and the statistical model of reference [17]. All models describe the general trend of the experimental data correctly. The microscopic models under-predict and the statistical model over-predicts the measured  $\Lambda/\pi$  ratios.

The  $\bar{\Lambda}/\Lambda$  ratio at mid-rapidity rises steeply from AGS [18] to RHIC energies [11,19,20] (see figure 4, left). The numerical values are  $0.027 \pm 0.0025$  for 40,  $0.079 \pm 0.01$  for 80 and  $0.149 \pm 0.016$  for 158 A·GeV, respectively. The same trend is measured for the  $\bar{p}/p$  ratio [21,22], but the numerical values are smaller than for the corresponding  $\bar{\Lambda}/\Lambda$  ratio. ( $0.0079 \pm 0.0008$ ,  $0.028 \pm 0.0025$ ,  $0.060 \pm 0.005$ , respectively). Total yields for p and  $\bar{p}$  will give more insight into this problem.

The  $\bar{\Lambda}/\bar{p}$  ratio allows to study the interplay of production and annihilation processes. In the SPS energy range this ratio indicates an increase with decreasing energy as illustrated in figure 4, right. The data at lower and higher energies are taken from [10,23,19].

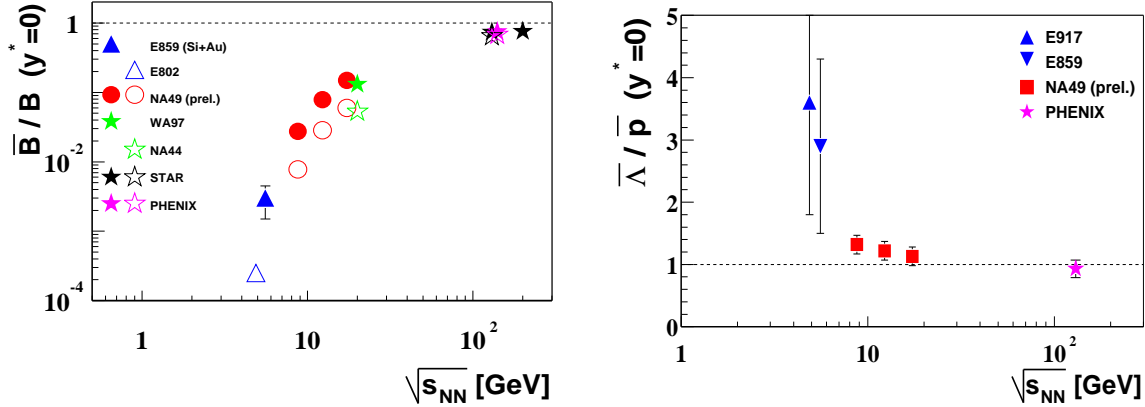


Figure 4. The  $\bar{\Lambda}/\Lambda$  (left) and  $\bar{\Lambda}/\bar{p}$  (right) ratio as a function of c.m. energy. All particles are corrected for weak decay feed-down.

In summary, the ratio  $\Lambda/\pi$  shows a maximum between top AGS energies and 40 A·GeV whereas the  $\bar{\Lambda}/\pi$  ratio increases monotonically with increasing energy. The upcoming measurements at 20 and 30 A·GeV will give more details for this energy range.

Acknowledgements: The author thanks E.L. Bratkovskaya, K. Redlich and N. Xu for providing the model predictions. This work was supported by the Director, Office of Energy Research, Division of Nuclear Physics of the Office of High Energy and Nuclear Physics of the US Department of Energy (DE-ACO3-76SFOOO98 and DE-FG02-91ER40609), the US National Science Foundation, the Bundesministerium für Bildung und Forschung, Germany, the Alexander von Humboldt Foundation, the UK Engineering and Physical Sciences Research Council, the Polish State Committee for Scientific Research (2 P03B 130 23 and 2 P03B 02418), the Hungarian Scientific Research Foundation (T14920 and T32293), Hungarian National Science Foundation, OTKA, (F034707), the EC Marie Curie Foundation, and the Polish-German Foundation.

## REFERENCES

1. M. Gaździcki, D. Röhrich, *Z. Phys. C*71, 55, 1996.
2. M. Gaździcki, M.I. Gorenstein, *Acta Phys. Polon.* B30, 2705, 1999.
3. S.V. Afanasiev *et al.* [NA49 Collaboration], *Nucl. Instrum. Meth.* A430, 210, 1999.
4. A. Mischke *et al.* [NA49 Collaboration], *J. Phys. G, Nucl. Part. Phys.* 28, 1761, 2002.  
A. Mischke, Ph.D. thesis, Univ. of Frankfurt, 2002.
5. S.V. Afanasiev *et al.* [NA49 Collaboration], *Phys. Rev. C*, submitted, 2002. (nucl-ex/0205002).
6. M. Gaździcki, D. Röhrich, *Z. Phys.* C65, 215–223, 1995.
7. J.L. Klay, PhD thesis, Univ. of California, Davis, 2001.
8. G. Rai *et al.* [E895 Collaboration], *Nucl. Phys.* A661, 162, 1999.
9. S. Albergo *et al.* [E896 Collaboration], *Phys. Rev. Lett.* 88, 062301, 2002.
10. B.B. Back *et al.* [E917 Collaboration], *Phys. Rev. Lett.* 87, 242301, 2001.
11. C. Adler *et al.* [STAR Collaboration], 2002, nucl-ex/0203016.
12. C. Pinkenburg *et al.* [E895 Collaboration], *Nucl. Phys.* A698, 495c, 2002.
13. F. Becattini *et al.*, *Phys. Rev. C*64, 024901, 2001.
14. H. Weber, E.L. Bratkovskaya, H. Stöcker, *submitted to Phys. Lett. B*, 2002. (nucl-th/0205030).

15. E.L. Bratkovskaya, private communication, 2002.
16. N. Xu, private communication, 2002.
17. P. Braun-Munzinger *et al.*, *Nucl. Phys.* A697, 902, 2002.
18. Y. Akiba *et al.* [E859 Collaboration], *Nucl. Phys.* A590, 179c, 1995.
19. K. Adcox *et al.* [PHENIX Collaboration], nucl-ex/0204007.
20. G. van Buren, *J. Phys. G, Nucl. Part. Phys.* 28, 2103, 2002.
21. L. Ahle *et al.* [E802 Collaboration], *Phys. Rev. Lett.* 81, 2650, 1998.
22. I. Bearden *et al.* [NA44 Collaboration], *Phys. Lett.* B471, 6, 1999.
23. G. Stephans *et al.* [E859 Collaboration], *J. Phys.* G23, 1895, 1997.